Transport properties of the fluid produced at Relativistic Heavy-Ion Collider

RAJEEV S BHALERAO

Department of Theoretical Physics, Tata Institute of Fundamental Research,
Homi Bhabha Road, Colaba, Mumbai 400 005, India
E-mail: bhalerao@tifr.res.in

Abstract. It is by now well known that the relativistic heavy-ion collisions at RHIC, BNL have produced a strongly interacting fluid with remarkable properties, among them the lowest ever observed ratio of the coefficient of shear viscosity to entropy density. Arguments based on ideas from the string theory, in particular the AdS/CFT correspondence, led to the conjecture – now known to be violated – that there is an absolute lower limit $1/4\pi$ on the value of this ratio. Causal viscous hydrodynamics calculations together with the RHIC data have put an upper limit on this ratio, a small multiple of $1/4\pi$, in the relevant temperature regime. Less well-determined is the ratio of the coefficient of bulk viscosity to entropy density. These transport coefficients have also been studied non-perturbatively in the lattice QCD framework, and perturbatively in the limit of high-temperature QCD. Another interesting transport coefficient is the coefficient of diffusion which is also being studied in this context. In this paper some of these recent developments are reviewed and then the opportunities presented by the anticipated LHC data are discussed, for the general nuclear physics audience.

1. Introduction

Transport coefficients of the QCD matter are of fundamental importance not only because they represent an important aspect of QCD, but also because they can be calculated from first principles. Trying to extract these coefficients reliably from experimental data and evaluating them in various theoretical approaches is a very active area of research today.

This review is addressed to the general nuclear physics audience, a majority of whom do not work in the area of relativistic heavy-ion collisions, but have probably heard the claim that the RHIC experiments have produced the most perfect fluid ever observed. Before the meaning of this claim is explained and the experimental evidence is presented for it, a few introductory remarks are in order. It may be recalled that the phase diagram (pressure vs. temperature) of the most familiar liquid, namely, water is known for long with good accuracy. In particular, the

coordinates of the triple point and the critical point are known to several significant places, and the various phase coexistence lines are well-determined. In contrast, the phase diagram of the strongly-interacting matter or the QCD phase diagram (temperature vs. the net baryon number density or equivalently the baryon number chemical potential) is known only schematically from the experimentalist's point of view. Indeed, the various phases that might occur at high densities are not known with certainty.

The big idea is to map out quantitatively the QCD phase diagram with the relativistic heavy-ion collisions as an experimental tool. Such experiments have been performed at SPS (CERN), are being performed at RHIC (BNL), and will soon be performed at LHC (CERN), at successively higher energies: up to $\sqrt{s}_{NN} = 19$, 200 and 5400 GeV, at the above three facilities, respectively. It is also necessary to systematically scan the energy range up to 200 GeV in order to study the QCD matter at high baryon number density and to locate the critical point and the phase transition line predicted by some theories. This is being done at RHIC and plans are afoot to do it at FAIR (GSI) and NICA (JINR).

In non-relativistic fluid dynamics, the kinematic viscosity (ν) is defined as $\nu = \eta/\rho$ where η is the coefficient of shear viscosity or the dynamic viscosity and ρ is the density of the fluid. It allows us to compare the viscosities of fluids with different densities. (Interestingly, under standard conditions, water has a lower ν than air, although its η is higher.) The dimensionless ratio η/s serves as the relativistic analog of the kinematic viscosity, s being the entropy density [1]. (The dimensionless ratio η/n where n is the number density is of no use here because n is ill-defined in relativistic heavy-ion collisions.)

Figure 1 shows η/s as a function of $(T-T_0)/T_0$ where T is the temperature and T_0 is the critical temperature, for various fluids, namely water, nitrogen, helium
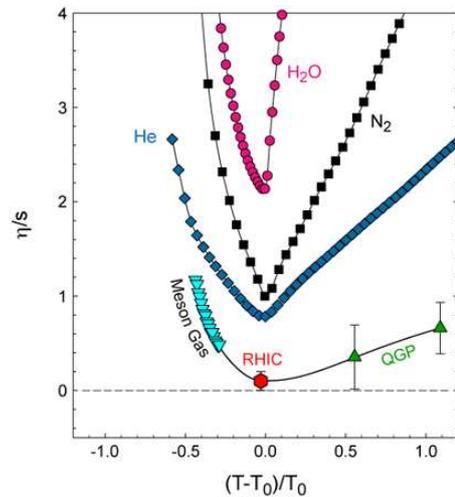

Figure 1. Comparison of different fluids with each other (see the text for details). The lines are drawn to guide the eye (figure reproduced from ref. [2]).

and the QCD matter. The three upper curves, drawn at the respective critical pressures, exhibit a cusp at T_0. The liquid and gaseous phases behave differently because the momentum transport mechanisms are different in the two cases (see, e.g., [3]). The points labelled Meson Gas have large ($\sim 50\%$) errors and are obtained from chiral perturbation theory. The points labelled QGP are from lattice QCD simulations of [4]. The point labelled RHIC is discussed below. This comparison of various fluids explains the statement that the RHIC fluid is the most perfect fluid ever observed.

The point labelled RHIC in figure 1 was obtained by matching the elliptic flow data at RHIC with the results of viscous hydrodynamic calculations: Consider a non-central collision of two identical spherical nuclei as shown in figure 2. The nuclei travel parallel to the z-axis, xy plane is called the azimuthal or transverse plane and xz plane is called the reaction plane. The overlap zone is shown as the shaded area in the figure. In an ultrarelativistic collision, the nucleons in the non-overlapping zones continue to travel more or less along their pre-collision trajectories, leaving behind the almond-shaped overlap zone. The interesting observables are governed mostly by the overlap zone which has a very high initial energy density. The spatial anisotropy of the overlap zone ensures anisotropic pressure gradients in the xy plane. This leads to a final state characterized by momentum anisotropy and anisotropic distribution of particles in the xy plane.

The triple differential invariant distribution of particles emitted in the final state is given by

$$E \frac{\mathrm{d}^3 N}{\mathrm{d}^3 p} = \frac{\mathrm{d}^3 N}{p_{\mathrm{T}} \, \mathrm{d}p_{\mathrm{T}} \, \mathrm{d}y \, \mathrm{d}\phi} = \frac{\mathrm{d}^2 N}{p_{\mathrm{T}} \, \mathrm{d}p_{\mathrm{T}} \, \mathrm{d}y} \frac{1}{2\pi} \left[1 + \sum_{1}^{\infty} 2v_n \cos(n\phi) \right],$$

where p_{T} is the transverse momentum, y is the rapidity and ϕ is the azimuthal angle of an emitted particle. The azimuthal distribution is Fourier-decomposed, and the leading coefficients v_1 and v_2 are called the directed and elliptic flow, respectively. They provide a measure of the anisotropy of the flow in the transverse plane, mentioned above. The importance of v_2 lies in the fact that it is a measure of pressure at early times and hence the measure of thermalization of the quark-gluon matter produced in heavy-ion collisions.
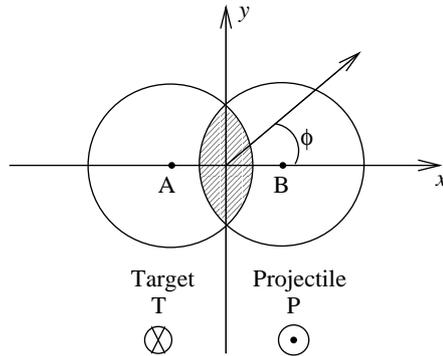

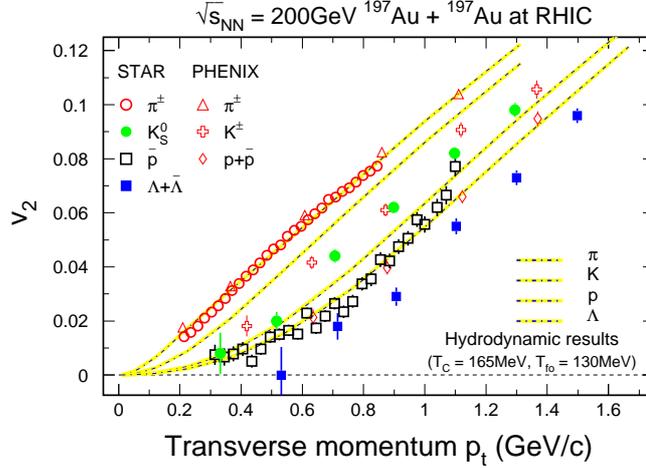**Figure 2.** Non-central collision of two nuclei.

Figure 3. Success of ideal hydrodynamics: Minimum-bias elliptic flow data compared with ideal hydrodynamics calculations of Huovinen (figure reproduced from ref. [5]).

Hydrodynamics is an effective theory that describes the slow, long-wavelength motion of a fluid close to equilibrium. It is a powerful technique because given the initial conditions and only the equation of state (EoS) of the matter, it predicts the space-time evolution of the fluid. Its limitation is that it is applicable at or near (local) thermodynamic equilibrium only. Hydrodynamics plays a central role in modelling relativistic heavy-ion collisions. State-of-the-art calculations for the RHIC data are based on the relativistic causal dissipative hydrodynamics. However, the initial calculations were done in the ideal ($\eta/s = 0$) hydrodynamics framework (see figure 3). The broad agreement between the data and these initial calculations, in particular the mass ordering of $v_2(p_{\mathrm{T}})$, led to the claim that the RHIC experiments have produced the most perfect fluid ever observed.

2. Transport coefficients

Consider a fluid in equilibrium. If it is perturbed so that the density is no longer uniform, it responds by setting up currents which tend to restore the equilibrium. In the linear response theory, the current or flux is proportional to the force which is negative of the gradient of the density: $\rho\mathbf{u} = -D\nabla\rho$. The constant of proportionality (D) is called the coefficient of diffusion. Other familiar examples are Ohm's law $\mathbf{J} = \sigma\mathbf{E} = -\sigma\nabla\phi$, Fourier's law of heat conduction $\mathbf{Q} = -\kappa\nabla T$, etc. A slightly more complicated example involves the transport of momentum in response to velocity gradients in an anisotropic medium, the constant of proportionality being the shear viscosity tensor. Such equations are called constitutive equations because they express physical properties of the material concerned. They relate the fluxes with the forces, the constants of proportionality being the transport coefficients.

Table 1. Various ways to calculate transport coefficients for relativistic fluids.

	Kinetic theory	Boltzmann equation
Weak-coupling regime	Linear-response theory	Kubo formula
	$N = 4$ Supersymmetric Yang–Mills theory	
	Lattice gauge theory	Kubo formula
Strong-coupling regime		
	$N = 4$ Supersymmetric Yang–Mills theory	

In addition to the variables such as the hydrodynamic four-velocity, pressure, energy density, conserved-number density, etc., hydrodynamics equations also contain transport coefficients (shear and bulk viscosities, thermal conductivity, relaxation times, etc.). These are external parameters which can be calculated in a variety of ways (see table 1) and fed into the hydrodynamics equations.

2.1 Transport coefficients from high-temperature QCD

High-temperature QCD assumes $T \gg \Lambda_{QCD}$. This is a weak-coupling regime and the shear (η) and bulk (ζ) viscosities can be calculated in the kinetic theory [6–8]:

$$\eta \sim \frac{T^3}{\alpha_s^2 \ln \alpha_s^{-1}}, \quad \zeta \sim \frac{\alpha_s^2 T^3}{\ln \alpha_s^{-1}}.$$

It is clear that as the temperature T rises, η/T^3 increases while ζ/T^3 decreases, and the ratio $\zeta/\eta \sim \alpha_s^4$ decreases. Note that the bulk viscosity vanishes for any conformal field theory, and QCD becomes conformal in the limit of high T. On the other hand, when $T \sim 200$ MeV, QCD is far from weakly coupled and the above results can provide only a rough estimate of η and ζ.

2.2 Transport coefficients from string theory

Like ordinary fluids, black holes too are thermal systems having notions of temperature and entropy. An object falling on the surface of a fluid in equilibrium generates disturbance which dies down due to the dissipative nature of the fluid. Similarly, the black hole horizon gets deformed when an object falls on it. However, it soon recovers its equilibrium shape. Thus the notion of 'viscosity' is applicable to a black hole as well, and the connection between hydrodynamics and black-hole physics does not seem very far-fetched.

Anti-de Sitter/conformal field theory (AdS/CFT) correspondence refers to the equivalence or duality between string theory defined on a certain AdS space and a CFT defined on its boundary. It allows the calculation of properties of a strongly-coupled CFT in terms of those of a weakly-coupled string theory. For an elementary introduction to these ideas, see [9].
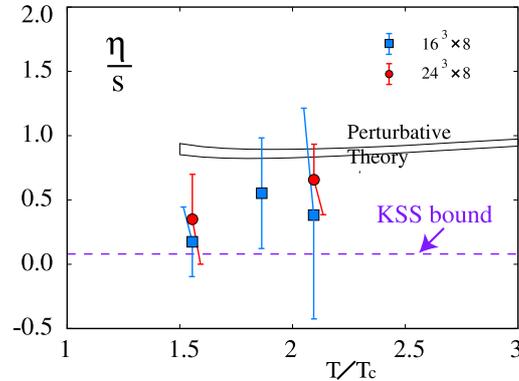
Figure 4. First lattice QCD results on η/s (figure reproduced from ref. [4]).

Ordinary quantum mechanics rules out vanishing η/s for weakly coupled theories, i.e., for theories with well-defined quasiparticles [10]. Kovtun *et al* [11], using string theory methods, showed that $\eta/s = 1/4\pi$, for a large class of strongly interacting quantum field theories whose dual description involves black holes in the anti-de Sitter (AdS) space. The value $1/4\pi$ was conjectured to be its absolute lower bound (KSS bound) for all substances. However, it has recently been realized that the KSS bound is violated for certain conformal field theories (CFT) [12,13].

Of course, applying the above ideas to the fluid produced at RHIC is speculative: QCD near the deconfinement transition temperature is not a CFT, and its gravity dual (if it exists) is not known.

2.3 *Transport coefficients from lattice QCD*

Figure 4 shows the results of a quenched QCD (i.e., no dynamical quarks or $m_q \to \infty$) calculation of η/s from ref. [4] in comparison with the high-T QCD results quoted in §2.1 and the KSS bound mentioned in the previous subsection. However, these initial results have now been superseded by more recent results described next.

Recently, Meyer has calculated both η/s and ζ/s on the lattice, with higher statistical accuracy and a more efficient algorithm, assuming $SU(3)$ gluodynamics [14,15]. He gets

$$\eta/s = \begin{cases} 0.134(33), & T = 1.65T_c, \\ 0.102(56), & T = 1.24T_c. \end{cases}$$

where the errors contain an estimate of the systematic uncertainty. This is consistent with the KSS bound. Further,

$$\zeta/s = \begin{cases} 0.008(7)\begin{bmatrix} 0.15 \\ 0 \end{bmatrix}, & T = 1.65T_c \\ 0.065(17)\begin{bmatrix} 0.37 \\ 0.01 \end{bmatrix}, & T = 1.24T_c \end{cases},$$

$$\zeta/s = 0.73(3)\begin{bmatrix} 2.0 \\ 0.5 \end{bmatrix}, \qquad T = 1.02T_c,$$

where the statistical error is given and the square bracket specifies conservative upper and lower bounds. Note the sharp rise in ζ/s just above T_c. Similar dramatic rise was seen in the results presented in [16] (see figure 5). They extracted the bulk viscosity in the presence of light quarks by combining low-energy theorems with lattice data on the QCD EoS. However, it is now realized that a determination of ζ from correlation functions of the energy–momentum tensor is more subtle. Shortcomings of this calculation have been pointed out in [17]. If the sharp rise of ζ/s just above T_c is confirmed, it would imply that the QGP is not a perfect fluid near T_c!

For a review of the progress made in extracting transport properties of the gluonic plasma from lattice simulations, see [18].

2.4 *Transport coefficients extracted from RHIC data*

Here the basic idea is that the shear viscosity reduces the elliptic flow: $v_2(\text{viscous fluid}) < v_2(\text{ideal fluid})$. This is easy to understand: recall that v_2 is a measure of the flow anisotropy in the azimuthal plane. Viscosity is the result of a frictional force. Frictional force being proportional to the flow velocity has a relatively stronger effect on fast-moving particles emerging in the reaction plane. This reduces the anisotropy and hence v_2.

Thus, if one has a good control on $v_2(\text{ideal fluid})$, one can adjust η/s to fit the data on v_2, and thus extract η/s. This has been done by several groups [19–25]. Results of [21] are shown in figure 6. The Glauber and colour-glass-condensate (CGC) initial conditions for hydrodynamic evolution yield $\eta/s \simeq 0.08$ and $\simeq 0.16$ respectively, showing the sensitivity of the extracted η/s to the initial conditions.
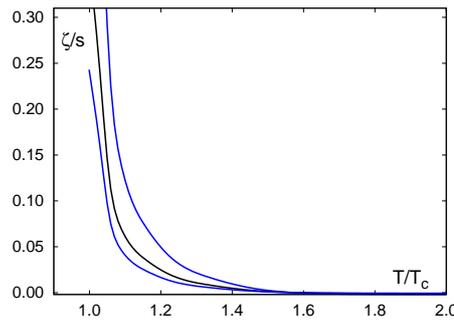

Figure 5. Bulk viscosity vs. temperature. The three curves (top to bottom) correspond to $\omega_0(T) = 0.5, 1, 1.5$ GeV respectively, where $\omega_0(T)$ is a scale at which the perturbation theory becomes valid. The three curves reflect the uncertainty in the determination of this scale parameter (figure reproduced from ref. [16]). See, however, the discussion in the text.
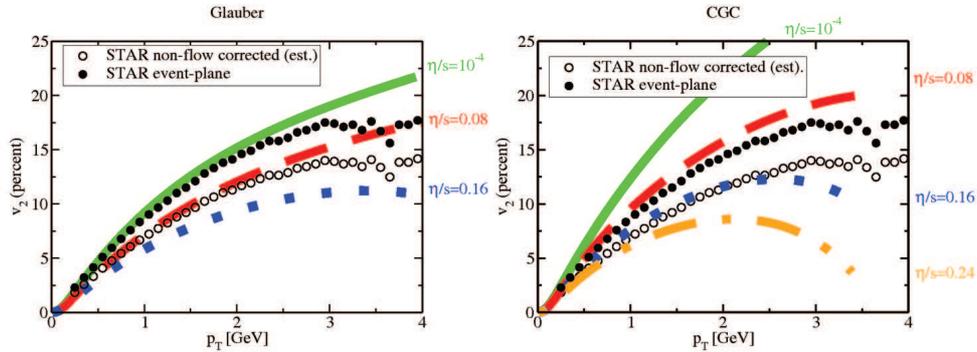
Figure 6. Minimum-bias elliptic flow data for charged hadrons in 200 GeV
Au–Au collisions (only statistical errors are shown). Line thickness is an
estimate of the accumulated numerical error (figure reproduced from ref. [21]).

Table 2. Various transport phenomena.

Transport of	By diffusion	By propagating waves	Experimental situation
Heat	Fourier's law	Maxwell–Cattaneo law	Second sound in superfluid He
Momentum	Navier–Stokes eq.	Maxwell–Cattaneo law	Propagating shear waves
Conserved no.	Fick's law	Kelly's law	RHIC?
e.g., B, Q, S			

3. Diffusion

Transport of heat occurs by diffusion (Fourier's law) as well as by propagating
waves (Maxwell–Cattaneo law). The latter mechanism underlies the well-known
phenomenon of second sound in superfluid helium (table 2). Similarly, the transport
of momentum too occurs by diffusion (Navier–Stokes equation) or by propagating
waves. These are the transverse or shear waves [26], different from the more familiar
longitudinal or compressional waves (for a detailed discussion, see [27]).

We recently studied the transport of a conserved number such as the net baryon
number (B), charge (Q), or strangeness (S) conserved in strong interactions, in the
acausal and causal, or the first- and second-order theories of relativistic diffusion
[28]. We found that Fick's diffusion smooths out gradients in the number density
monotonically. In contrast, in Kelly's theory the gradients may be transiently am-
plified, i.e., the density profile may stiffen at intermediate times (see figure 7). We
proposed experimental observables and argued that the RHIC data can potentially
distinguish between the above two mechanisms. If the second-order theory of dif-
fusion is ruled out by the data, one gets a handle on the relaxation time and hence
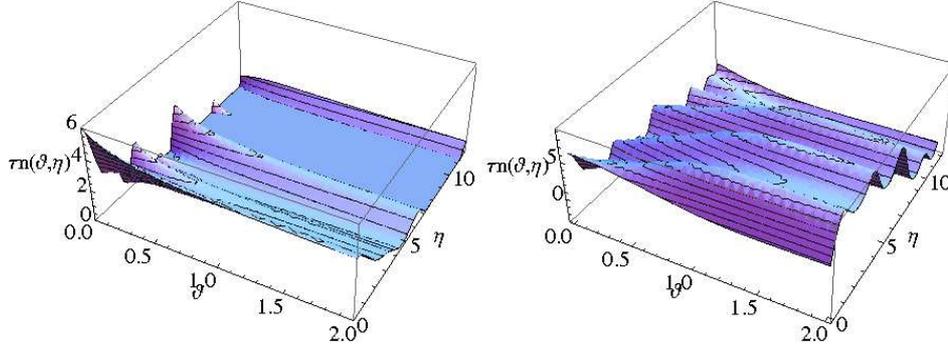on thermalization.

Figure 7. Conserved number density profile as a function of time and space-time rapidity in the Fick (left) and Kelly (right) theories of diffusion (figure reproduced from ref. [28]).

Table 3. Comparison of central Au–Au collisions at RHIC and central Pb–Pb collisions at LHC.

	RHIC (Au–Au)	LHC (Pb–Pb)
$\sqrt{s}_{NN}$	200 GeV	5.5 TeV
Initial temperature	$\sim 2T_c$	$\sim 4T_c$
Initial energy density	~ 5 GeV/fm^3	15–60 GeV/fm^3
Lifetime	~ 10 fm/c	>10 fm/c

4. Viscosity in ordinary finite nuclei

This review is about the transport properties of the fluid produced at RHIC. But it is pertinent to ask what do we know about the transport coefficients of the matter in an ordinary finite nucleus at low temperatures. Hydrodynamic models have a long history in nuclear physics – recall the success of the liquid drop model. The coefficient of shear viscosity of a finite nucleus can be obtained from (i) analysis of the widths of giant resonances within the hydrodynamic model (ii) the process of fission studied within the liquid drop model and (iii) kinetic theory. This has been discussed recently in [29]. Using entropy density for a free Fermi gas or for non-interacting nucleons in a Woods–Saxon potential, they obtained values of η/s larger than but not drastically different from those for the RHIC fluid.

5. What about LHC?

It is clear from table 3 that at LHC we would need η/s and ζ/s up to $T \sim 4T_c$. Some preliminary lattice results are now available, but for the $SU(3)$ pure gauge theory (i.e., quarkless QCD) [18]. For a careful extraction of η/s and ζ/s from LHC (and RHIC) data, we need to incorporate the T-dependence of these transport coefficients

in hydrodynamic calculations, among other refinements of these calculations; see the next section.

6. Take-home message

- Elliptic flow at RHIC has put a robust upper limit on the value of η/s of the RHIC fluid: $\eta/s \lesssim 5/(4\pi)$. This is the average value in the relevant temperature region.
- Uncertainties associated with the initial conditions, EoS, bulk viscosity, hadronic stage, freeze-out procedure and different versions of the second-order hydrodynamic equations prevent a more precise determination of η/s (see ref. [30] for a detailed discussion).
- The bulk viscosity is not yet well-determined in the deconfinement transition region.
- Analysis of the RHIC data, which might throw light on the coefficient of diffusion, is awaited.

Acknowledgments

References

[1] Strictly speaking, relativistic analog of ρ is $(\epsilon + P) = sT$ where ϵ is the energy density and P the pressure
[2] R A Lacey *et al*, *Phys. Rev. Lett.* **98**, 092301 (2007)
[3] L P Csernai, J I Kapusta and L D McLerran, *Phys. Rev. Lett.* **97**, 152303 (2006)
[4] A Nakamura and S Sakai, *Phys. Rev. Lett.* **94**, 072305 (2005)
[5] STAR Collaboration: M D Oldenburg, *J. Phys.* **G31**, S437 (2005)
[6] P Arnold, G D Moore and L G Yaffe, *J. High Energy Phys.* **0011**, 001 (2000)
[7] P Arnold, G D Moore and L G Yaffe, *J. High Energy Phys.* **0305**, 051 (2003)
[8] P Arnold, C Dogan and G D Moore, *Phys. Rev.* **D74**, 085021 (2006)
[9] M Natsuume, arXiv:hep-ph/0701201
[10] P Danielewicz and M Gyulassy, *Phys. Rev.* **D31**, 53 (1985)
[11] P Kovtun, D T Son and A O Starinets, *Phys. Rev. Lett.* **94**, 111601 (2005)
[12] A Buchel, R C Myers and A Sinha, *J. High Energy Phys.* **0903**, 084 (2009)
[13] M Brigante, H Liu, R C Myers, S Shenker and S Yaida, *Phys. Rev. Lett.* **100**, 191601 (2008)
[14] H B Meyer, *Phys. Rev.* **D76**, 101701 (2007)
[15] H B Meyer, *Phys. Rev. Lett.* **100**, 162001 (2008)
[16] F Karsch, D Kharzeev and K Tuchin, *Phys. Lett.* **B663**, 217 (2008)
[17] K Huebner, F Karsch and C Pica, *Phys. Rev.* **D78**, 094501 (2008)
[18] H B Meyer, *Nucl. Phys.* **A830**, 641C (2009)
[19] R J Fries, B Muller and A Schafer, *Phys. Rev.* **C78**, 034913 (2008)

[20] P Romatschke and U Romatschke, *Phys. Rev. Lett.* **99**, 172301 (2007)
[21] M Luzum and P Romatschke, *Phys. Rev.* **C78**, 034915 (2008), Erratum, *ibid.* **C79**, 039903 (2009)
[22] H Song and U W Heinz, *Phys. Rev.* **C77**, 064901 (2008)
[23] K Dusling and D Teaney, *Phys. Rev.* **C77**, 034905 (2008)
[24] D Molnar and P Huovinen, *J. Phys.* **G35**, 104125 (2008)
[25] A K Chaudhuri, *Phys. Lett.* **B681**, 418 (2009)
[26] They are used, e.g., in magnetic resonance elastography (MRE) for quantitatively imaging the material properties
[27] P Romatschke, arXiv:0902.3663 [hep-ph]
[28] R S Bhalerao and S Gupta, *Phys. Rev.* **C79**, 064901 (2009)
[29] N Auerbach and S Shlomo, *Phys. Rev. Lett.* **103**, 172501 (2009)
[30] U W Heinz, J S Moreland and H Song, *Phys. Rev.* **C80**, 061901 (2009)